RESEARCH ARTICLE

Effects of shell morphology on mechanics of zebra and quagga mussel locomotion

Suzanne M. Peyer[1],*, John C. Hermanson[2] and Carol Eunmi Lee[1,3]

[1]Department of Zoology, University of Wisconsin, Madison, WI 53706, USA, [2]US Forest Service, Forest Products Laboratory, Madison, WI 53726, USA and [3]Center of Rapid Evolution (CORE), 430 Lincoln Drive, Birge Hall, University of Wisconsin, Madison, WI 53706, USA

*Author for correspondence (smpeyer@wisc.edu)

SUMMARY

Although zebra mussels (*Dreissena polymorpha*) initially colonized shallow habitats within the North American Great Lakes, quagga mussels (*Dreissena bugensis*) are becoming dominant in both shallow- and deep-water habitats. Shell morphology differs among zebra, shallow quagga and deep quagga mussels but functional consequences of such differences are unknown. We examined effects of shell morphology on locomotion for the three morphotypes on hard (typical of shallow habitats) and soft (characteristic of deep habitats) sedimentary substrates. We quantified morphology using the polar moment of inertia, a parameter used in calculating kinetic energy that describes shell area distribution and resistance to rotation. We quantified mussel locomotion by determining the ratio of rotational (K_{rot}) to translational kinetic energy (K_{trans}). On hard substrate, K_{rot}:K_{trans} of deep quagga mussels was fourfold greater than for the other morphotypes, indicating greater energy expenditure in rotation relative to translation. On soft substrate, K_{rot}:K_{trans} of deep quagga mussels was approximately one-third of that on hard substrate, indicating lower energy expenditure in rotation on soft substrate. Overall, our study demonstrates that shell morphology correlates with differences in locomotion (i.e. K_{rot}:K_{trans}) among morphotypes. Although deep quagga mussels were similar to zebra and shallow quagga mussels in terms of energy expenditure on sedimentary substrate, their morphology was energetically maladaptive for linear movement on hard substrate. As quagga mussels can possess two distinct morphotypes (i.e. shallow and deep morphs), they might more effectively utilize a broader range of substrates than zebra mussels, potentially enhancing their ability to colonize a wider range of habitats.

Key words: biological invasions, bivalve, functional morphology, Great Lakes, kinetic energy, locomotion, mollusc, moment of inertia, sediment.

INTRODUCTION

Zebra mussels (*Dreissena polymorpha* Pallas 1771) and quagga mussels (*Dreissena bugensis* Andrusov 1897) are two highly invasive species that have become established in the Great Lakes of North America within the past 25 years (Gelembiuk et al., 2006; Karatayev et al., 1998; May et al., 2006), causing much ecological destruction and economic loss (Pimentel et al., 2005). Although zebra mussels have inflicted negative ecological impacts as the earlier colonizer, quagga mussels might eventually become more widespread and destructive than zebra mussels. Quagga mussels initially became prevalent in deep (>50 m) soft sedimentary habitats (e.g. sand, silt), where zebra mussels tend to be rare (Dermott and Munawar, 1993; Mills et al., 1993). However, quagga mussels have more recently been displacing zebra mussels in shallow (<15 m) hard substrate habitats (e.g. rocks and mollusc shells), where zebra mussels previously had been more dominant (Jarvis et al., 2000; Mills et al., 1996; Mills et al., 1999; Stoeckmann, 2003). Differences in shell morphology between zebra and quagga mussels have been proposed to contribute to differences in their ability to colonize diverse substrate types among habitats (e.g. shallow hard *versus* deep soft sedimentary substrates), potentially affecting competition between the two species (Claxton et al., 1998; Peyer et al., 2010). However, functional consequences of the morphological differences had not been thoroughly examined.

Zebra mussels possess only a shallow-water morphotype, whereas quagga mussels have distinct shallow- and deep-water morphotypes (Fig. 1) (Claxton et al., 1998; Dermott and Munawar, 1993; Peyer et al., 2010). Differences in shell morphology between shallow- and deep-water quagga mussels were found to result from phenotypic plasticity, rather than genetic differentiation, in a common-garden experiment in which the mussels were reared under various environmental conditions (Peyer et al., 2010). Although zebra and shallow quagga mussels resemble each other in overall shell morphology (Fig. 1A *versus* 1B) [e.g. in terms of shell height to width ratio (Claxton et al., 1998)], they differ in ventral surface morphology, which is distinctly flattened for zebra mussels and slightly rounded for shallow quagga mussels (Fig. 1A *versus* 1B, anterior–posterior views) (Claxton et al., 1998; Dermott and Munawar, 1993). In contrast to zebra and shallow quagga mussels (Fig. 1A,B), deep quagga mussels (Fig. 1C) have shells that are more flattened and compressed together (Fig. 1C, dorsal–ventral view), more ovular in shape (Claxton et al., 1998; Dermott and Munawar, 1993; Peyer et al., 2010) and less dense (Claxton et al., 1998; Roe and MacIsaac, 1997). The ventral surface morphology of deep quagga mussels (Fig. 1C, anterior–posterior view) is much more pointed than that of zebra and shallow quagga mussels (Fig. 1A,B, anterior–posterior views). Such differences in shell morphology among the three morphotypes (Fig. 1) have been suggested to affect their interaction with different substrate types, influencing the distribution of each species within the Great Lakes (Claxton et al., 1998; Dermott and Munawar, 1993; Mackie, 1991; Roe and MacIsaac, 1997) (see Discussion).
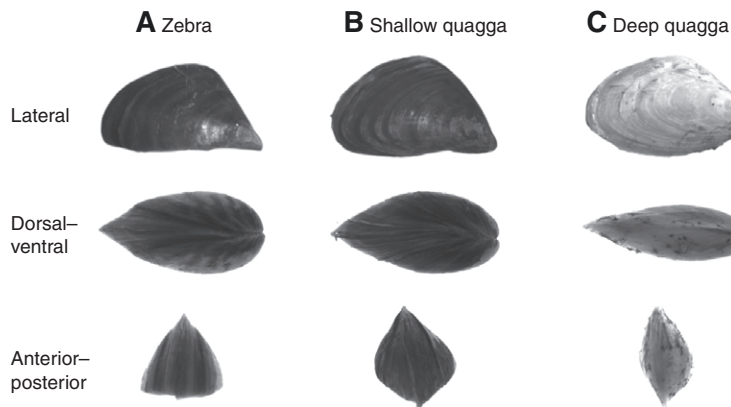
Fig. 1. Lateral, dorsal–ventral and anterior–posterior shell views of (A) zebra, (B) shallow quagga and (C) deep quagga mussels. Shells were 2–3 cm in length.

A shell morphology that facilitates locomotion across particular substrate types might affect fitness and survival of zebra and quagga mussels on those substrates. Zebra mussels are known to move in response to various environmental factors (e.g. light, nitrogenous waste, oxygen and substrate type) that influence habitat selection and survival (see Burks et al., 2002; Kilgour and Mackie, 1993; Kobak, 2001; Kobak and Nowacki, 2007; Marsden and Lansky, 2000; Toomey et al., 2002).

The objective of this study was to directly examine the effects of shell morphology on locomotion of different mussel morphotypes (i.e. zebra, shallow quagga and deep quagga mussels) on hard *versus* soft sedimentary substrates. We determined the effects of shell shape on locomotory function by calculating translational and rotational kinetic energy (K_{trans} and K_{rot}, respectively) for zebra and quagga mussels moving across hard and soft substrate types. K_{trans} and K_{rot} directly account for effects of shell size and shape on locomotory function, as K_{trans} is a function of mussel mass and velocity whereas K_{rot} is a function of mussel mass moment of inertia and angular velocity. For the mass moment of inertia of the mussel, we used as a surrogate the polar moment of inertia (see Peyer et al., 2010), which was our descriptor of shell morphology. Thus, K_{rot} includes specific information on shell morphology, allowing us to observe direct links between shell shape and locomotion.

Although moments of inertia have been used in studies of animal locomotion, they have often been applied to specific anatomical features (e.g. vertebrate limbs) rather than to whole-animal morphology and locomotion (e.g. Walter and Carrier, 2002; Carrier et al., 2001). In contrast to previous studies that examined locomotion of rigid-bodied (i.e. shelled) animals (e.g. Alexander, 1993; Amyot and Downing, 1998; Uryu et al., 1996; Waller et al., 1999), we quantified whole-shell morphology using the polar moment of inertia, and then directly linked this geometrical measure to the mechanics of mussel locomotion. This approach enabled us to directly observe the relationship between zebra and quagga mussel shell shape and locomotion.

MATERIALS AND METHODS
Population sampling
To quantify shell morphology, we collected zebra and quagga mussels 5–30 mm in size from Lake Ontario, North America. We collected the zebra and shallow quagga mussels in June 2006 from rocky substrate (1–2 m depth) in Oswego Harbor, NY, USA (~43°47′N, 76°49′W). We randomly sampled and removed mussels from rocks by cutting their byssal threads with a knife. We collected deep quagga mussels in April 2005 at Thirty Mile Point (43°24′N,

78°33′W), offshore from Niagara Falls, NY, USA, with a motor driven ponar grab (65 m depth).

We also collected zebra and quagga mussels in July 2008 from Lake Michigan, North America, for the analysis of movement across hard and soft sedimentary substrates. We collected zebra and shallow quagga mussels from several submerged poles made of polyvinyl chloride (1–3 m depth) at the University of Wisconsin Great Lakes WATER Institute in Milwaukee, WI, USA (~43°04′N, 87°95′W), stationed on the shore of Lake Michigan. We randomly sampled and removed these mussels from the poles by cutting their byssal threads with a knife. We collected deep quagga mussels offshore from Milwaukee, WI, USA (43°01′N, 87°21′W) using a trawl (60 m depth).

After collection, we wrapped mussels in damp paper towels and transported them on ice within sealed plastic bags. In the laboratory, we fed mussels a commercial shellfish diet (*Isochrysis* sp., *Pavlova* sp., *Tetraselmis* sp. and *Thalassiosira weissflogii*) from Reeds Mariculture Inc. (Campbell, CA, USA), an algal mixture that has been used to support zebra and quagga mussels previously (Vanderploeg et al., 1996; Peyer et al., 2009; Peyer et al., 2010). We housed mussels in aquaria at an experimental temperature range of ~18–20°C. Throughout this study we used water collected from Lake Michigan, at Racine Harbor, WI, USA, where both zebra and quagga mussels occur.

Collection of morphometric data
We digitally imaged zebra, shallow quagga and deep quagga mussels to quantify differences in shell morphology among the three morphotypes from Lake Ontario. We captured images of lateral, dorsal–ventral and anterior–posterior shell views of each mussel (Fig. 1) with a Dragonfly IEEE-1394 digital camera (Point Grey Research, Vancouver, BC, Canada). To quantify shell morphology, we used IMAQ programming software in LabVIEW (National Instruments, Austin, TX, USA) to obtain the polar moment of inertia as a surrogate for the mass moment of inertia of a mussel. The mass moment of inertia is a physical measurement that describes the distribution of the mass of an object and its resistance to rotation about an arbitrary axis (Hibbeler, 1989). The mass moment of inertia, I_{aa}, about an arbitrary axis, a, is defined as:

$$I_{aa} = \int_V \left\| \mathbf{u}_a \times \mathbf{r} \right\|^2 \rho(\mathbf{r}) \, dV \; , \qquad (1)$$

where $\mathbf{u}_a$ is the unit vector defining the a-axis, $\mathbf{r}$ is the vector from the a-axis to a differential element of the object volume, dV, and $\rho(\mathbf{r})$ is the density of the object at position $\mathbf{r}$ relative to the a-axis.
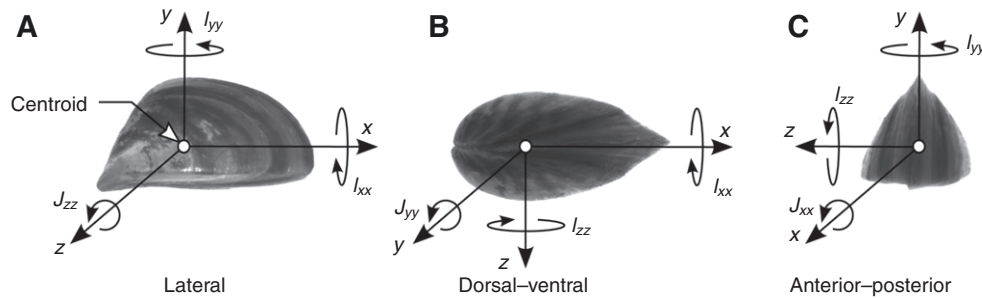
Fig. 2. Three shell views that were morphologically analyzed for zebra, shallow quagga and deep quagga mussels. (A) Lateral view (mussel's hinge at left, siphon at right): moments of inertia, I_{xx} and I_{yy}, were about the x- and y-axes and polar moment of inertia (J_{zz}) was about the z-axis (out of page). (B) Dorsal–ventral view (hinge at left, siphon at right, foot parallel to the page): moments of inertia, I_{xx} and I_{zz}, were about the x- and z-axes and polar moment of inertia (J_{yy}) was about the y-axis (out of page). (C) Anterior–posterior view (hinge and siphon were aligned with the x-axis, perpendicular to the page): moments of inertia, I_{yy} and I_{zz}, were about the y- and z-axes and polar moment of inertia (J_{xx}) was about the x-axis (out of page).

Greater distribution of mass for an object (greater I_{aa}) results in greater resistance to rotation, analogous to a spinning figure skater that has greater resistance to rotation and spins more slowly with outstretched arms than with arms held close to the body (i.e. lesser distribution of mass and lesser I_{aa}). In our study, we simplified the three-dimensional morphology reconstruction by using two-dimensional images of mussel shells, and by assuming the density distribution, $\rho(\mathbf{r})$, and thickness of mussels to be constants. With these assumptions, we simplified I_{aa} in Eqn 1 to the mussel mass multiplied by the polar moment of inertia (Fig. 2). We established a local orthogonal coordinate system on the mussel with the origin at its centroid and with the unit vector defined along the principal axis as calculated by the moment of inertia. Thus, for the lateral shell view (Fig. 2A), the polar moment of inertia about the z-axis, J_{zz}, (coming out of the page) at the shell centroid would then be defined by:

$$I_{aa} = m \cdot J_{zz} = m \cdot \int_A r_z^2 \, dA \, , \tag{2}$$

where r_z is the distance from the centroid to an element of the shell area, dA, and m is the mass of the mussel (see also Peyer et al., 2010). J_{zz} describes the distribution of the shell area and, assuming that $\rho(\mathbf{r})=m/V$ (V is shell volume) (Eqn 1), its resistance to rotation about the z-axis. Thus, a mussel with larger shell area has greater resistance to rotation than a mussel of smaller shell area for the same total mass.

Using LabVIEW, we calculated J_{zz} as the sum of the moments of inertia, I_{xx} and I_{yy}, about the centroid (see Beer and Johnston, 1981). From a two-dimensional perspective, I_{xx} and I_{yy} are the resistances of the shell area to rotation about the principal x- and y-axes, respectively, which intersect at the centroid (Fig. 2A) (Beer and Johnston, 1981). I_{xx} and I_{yy} are defined by the equations:

$$I_{xx} = \int_A y^2 \, dA \tag{3}$$

and

$$I_{yy} = \int_A x^2 \, dA \, , \tag{4}$$

respectively, where y and x are the distances from the x- and y-axes to dA.

We calculated polar moments of inertia for the dorsal–ventral and anterior–posterior shell views in the same manner as described above for the lateral shell view. For the dorsal–ventral shell view, we calculated J_{yy} about the y-axis as the sum of I_{xx} and I_{zz} (Fig. 2B),

and for the anterior–posterior shell view, we calculated J_{xx} about the x-axis as the sum of I_{yy} and I_{zz} (Fig. 2C). We captured images of the three shell views for mussels of various size (5–30 mm length), 60 per morphotype. We weighed all mussels because mass is used to calculate the mass moment of inertia (Eqn 2).

Analysis of morphometric data
We performed an analysis of covariance (ANCOVA), using the statistical package R (R Development Core Team, 2008), to test whether the polar moment of inertia depended on mussel morphotype (i.e. zebra, shallow quagga and deep quagga) and mussel mass. Our models for the polar moments of inertia for each shell view, J_{zz}, J_{yy} and J_{xx}, as dependent variables were:

$$J_{zz} = \beta_0 + \beta_1 x_t + \beta_2 x_m \, , \tag{5}$$

$$J_{yy} = \beta_0 + \beta_1 x_t + \beta_2 x_m \, , \tag{6}$$

and

$$J_{xx} = \beta_0 + \beta_1 x_t + \beta_2 x_m \, , \tag{7}$$

where independent variables were mussel morphotype (x_t) and mussel mass (x_m). Maximum likelihood parameter estimates were represented by β_0, β_1 and β_2. All variables were treated as fixed effects. As mass is a function of length cubed and moment of inertia is a function of length quartic, we raised mussel mass to the 4/3 power in order to non-dimensionalize its relationship with polar moments of inertia. Following the ANCOVA, we performed pairwise comparisons of J_{zz}, J_{yy} and J_{xx} between morphotypes.

Collection of mussel locomotion data
We examined zebra, shallow quagga and deep quagga mussel movement across either hard glass or soft sedimentary substrates. For this analysis, we used mussels collected from Lake Michigan. We observed mussels in two treatments, either in 20 liters aquaria with a 3 cm soft sediment layer or in aquaria without sediment, exposing a glass bottom. The aquaria were filled with ~10 liters of Lake Michigan water and gently aerated. The sedimentary substrate was collected from Lake Ontario with a motor driven ponar grab (65 m depth) in April 2005 at Thirty Mile Point, where we collected the deep quagga mussels. For the hard substrate treatment, we used the glass bottom of the aquarium because its surface was level, uniform and had low friction relative to the sedimentary substrate. Using glass enabled us to quantify movement on a flat hard surface alone without the extraneous
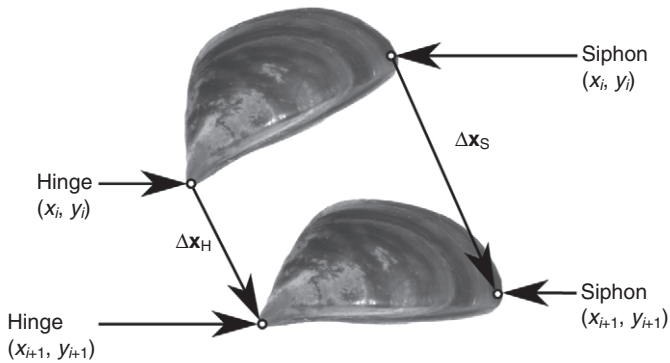
Fig. 3. Characterization of mussel movement between two imaging frames, with lateral shell surface parallel to the substrate. Coordinates (x, y) of the shell hinge and siphon were obtained, frame by frame, for each step taken by a mussel during its entire walk. These coordinates were used to quantify the displacement of the mussel hinge ($\Delta\mathbf{x}_H$) and siphon ($\Delta\mathbf{x}_S$) between frames.

Fig. 4. Variables used to calculate translational [$K_{trans}=1/2(m\cdot\mathbf{v}_c^2)$] and rotational kinetic energy [$K_{rot}=1/2(\mathbf{J}\cdot\boldsymbol{\omega}_c^2)$]. Images of mussel movement were captured once per minute. Thus, mussel velocity ($\mathbf{v}_c$) in the calculation of K_{trans} was defined as displacement, $\Delta\mathbf{x}_c$, in cm min^{-1} of the centroid and mussel angular velocity ($\boldsymbol{\omega}_c$) in the calculation of K_{rot} was defined as $\Delta\theta$ in rad min^{-1}.

effects of jagged or unlevel surfaces (e.g. rocks and mollusc shells) that would make the interaction with the hard surface more difficult to observe clearly. For both treatments, we placed six mussels of the same morphotype into each aquarium (five to 14 replicates per morphotype per substrate type), with the lateral shell view (Fig. 2A) towards (i.e. z-axis normal to) the substrate. We distributed the mussels, with roughly equal spacing, across each substrate. We used mussels of medium size (10–20 mm length, 0.3–0.8 g). Zebra and quagga mussels move across a substrate by pushing themselves with their foot, which extends out of their shells from their ventral surface. We captured images of mussels moving across each substrate with a Dragonfly IEEE-1394 digital camera and IMAQ programming software in LabVIEW at a rate of 1 frame min^{-1}. We recorded images over a 20 h period under dim light produced with a red 25 W bulb. The red bulb provided sufficient light for imaging the mussels, while providing limited visible spectrum, which mussels were found to prefer over white light conditions (Kobak, 2001; Kobak and Nowacki, 2007; Toomey et al., 2002). After each imaging session, we collected data on shell morphometrics and mussel mass as described above. We placed six mussels in each experimental replicate (i.e. six mussels per morphotype per substrate type). However, not all mussels moved during the observation period, resulting in a different number of observations per treatment. For those mussels moving on soft sedimentary substrate, we collected data on zebra mussels (N=24 total) from five replicate aquaria, shallow quagga mussels (N=24 total) from five replicate aquaria and deep quagga mussels (N=24 total) from nine replicate aquaria. For those mussels moving on hard substrate, we collected data on zebra mussels from nine replicate aquaria (N=32 total), shallow quagga mussels from seven replicate aquaria (N=30 total) and deep quagga mussels from 14 replicate aquaria (N=26 total).

We used time-lapse photographic images to quantify movement of mussels in translation and rotation. For each series of images of individual mussels moving across a given substrate, we used IMAQ programming software in LabVIEW to obtain x- and y-coordinates of the hinge and siphon of each mussel frame by frame (Fig. 3). With these coordinates we quantified translational and rotational movement of each mussel during an entire 'walk' within each 20 h imaging period. Translational movement is the displacement vector ($\Delta\mathbf{x}$) of the centroid of the mussel shell from frame to frame, whereas rotational movement is the angle vector ($\Delta\theta$) of the hinge-siphon
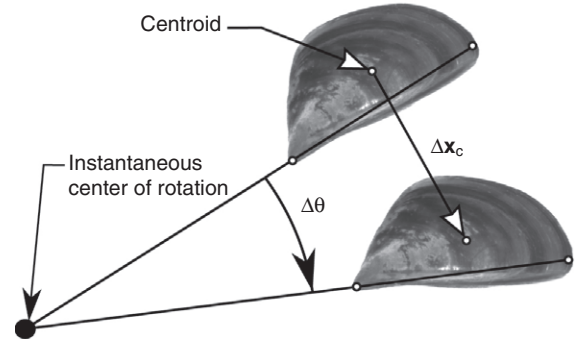
axis of the mussel shell from frame to frame (Fig. 4). Using $\Delta\mathbf{x}$, we calculated translational kinetic energy of mussels, K_{trans}, as:

$$K_{trans} = \frac{1}{2}m\cdot\mathbf{v}_c^2 \ , \qquad (8)$$

where m is the mussel mass and $\mathbf{v}_c$ is the velocity vector of the centroid of the mussel shell (i.e. $\Delta\mathbf{x}$ per frame, expressed in cm min^{-1} and representing one step per walk) (Hibbeler, 1989). We summed K_{trans} over the entire walk. Using $\Delta\theta$, we calculated rotational kinetic energy, K_{rot}, as:

$$K_{rot} = \frac{1}{2}m\cdot\boldsymbol{\omega}_c^T\cdot\mathbf{J}\cdot\boldsymbol{\omega}_c \ , \qquad (9)$$

where

$$\mathbf{J} = \begin{bmatrix} J_{xx} & 0 & 0 \\ 0 & J_{yy} & 0 \\ 0 & 0 & J_{zz} \end{bmatrix} \qquad (10)$$

and

$$\boldsymbol{\omega} = \begin{bmatrix} \omega_x \\ \omega_y \\ \omega_z \end{bmatrix} . \qquad (11)$$

The angular velocity vector ($\boldsymbol{\omega}$) was about the centroid of the mussel (i.e. $\Delta\theta$ in rad min^{-1}) (Hibbeler, 1989). We summed K_{rot} over a mussel's entire walk. For calculations of K_{trans} and K_{rot} we used data only for the time period during which a mussel was unobstructed by neighboring mussels or by walls of the aquarium.

In order to calculate the rotational kinetic energy, we determined the orientation of each mussel for each frame of an entire walk. While in motion, a mussel was able to position itself in different orientations (local reference frame) with respect to the substrate (global reference frame). We defined these orientations as the lateral, dorsal–ventral and anterior–posterior shell views (Fig. 1). It was important to determine the orientation of each mussel for calculating rotational kinetic energy (Eqn 9), because the variable, $\mathbf{J}$, differed for each shell view. Thus, in Eqn 9, $\mathbf{J}$ was a principal moments tensor that consisted of one of J_{zz}, J_{yy} or J_{xx} and was represented by a 3×3 matrix (Fig. 5; Eqn 10), indicating changes in orientation. For example, if at time T_i a mussel was positioned on its lateral
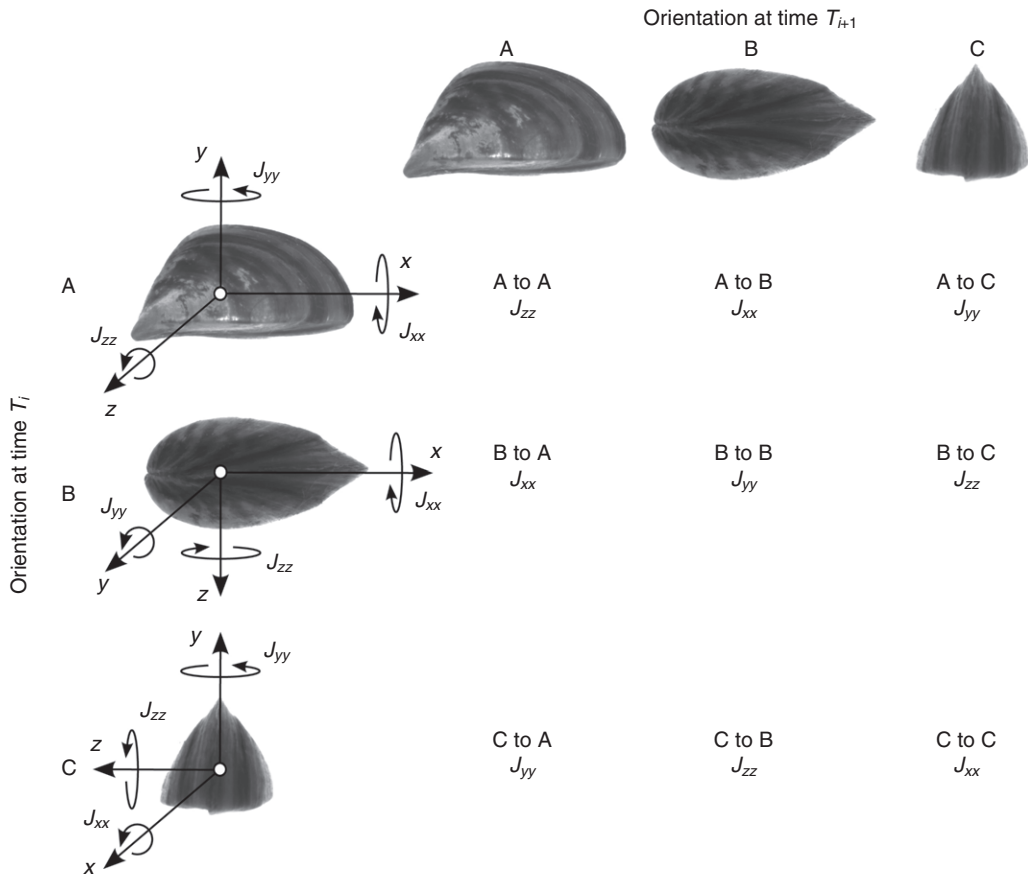
Orientation at time T_{i+1}

Fig. 5. Matrix of possible changes in mussel orientation during movement across a substrate. A mussel could rotate from being positioned on its (A) lateral, (B) ventral or (C) posterior surface at time T_i to being positioned on its (A) lateral, (B) ventral or (C) posterior surface at time T_{i+1}. In the process of moving from one position to another, a mussel rotated about different axes. The polar moments of inertia that were used as a mussel rotated from an orientation at T_i to another orientation at T_{i+1} are indicated in each cell of the matrix. For example, movement of a mussel from the lateral to the lateral surface (A to A) used J_{zz} of the lateral shell view, from lateral to ventral surface (A to B) used J_{xx} of the anterior–posterior shell view and from lateral to posterior surface (A to C) used J_{yy} of the dorsal–ventral shell view.

surface, at T_{i+1} it could have rotated about the z-axis (yawed) and remained positioned on its lateral surface (Fig. 5, A to A), rotated about the x-axis (rolled) onto its ventral surface (Fig. 5, A to B) or rotated about the y-axis (pitched) onto its posterior surface (i.e. hinge; Fig. 5, A to C).

Analysis of mussel locomotion

We characterized mussel locomotion using the ratio of rotational to translational kinetic energy ($K_{rot}{:}K_{trans}$), mean $\boldsymbol{\omega}^2$ to mean $\mathbf{v}_c^2$ ($\boldsymbol{\omega}^2{:}\mathbf{v}_c^2$) and net to total distance traveled (i.e. effective distance). We tested for differences in these values among the three morphotypes using ANOVA in the software package R. Mussels with high $K_{rot}{:}K_{trans}$ values expended more energy in rotational relative to translational movement. By using $K_{rot}{:}K_{trans}$ in our analyses rather than mean values for K_{rot} and K_{trans}, we normalized energy expenditure across all mussels. This normalization was necessary in order to determine the effect of shell morphology on locomotion, because individual mussels moved different distances, in turn affecting mean values for K_{rot} and K_{trans}. We also tested for differences in the $\boldsymbol{\omega}^2{:}\mathbf{v}_c^2$ ratio to determine the extent to which this value might have affected $K_{rot}{:}K_{trans}$. For example, a high value for $K_{rot}{:}K_{trans}$ could result from a high degree of turning relative to translating (i.e. high $\boldsymbol{\omega}^2{:}\mathbf{v}_c^2$ ratio) or from a large polar moment of inertia (the measure we used to characterize morphology) for a given mussel mass (see Eqns 8, 9). Therefore a significant effect of the $\boldsymbol{\omega}^2{:}\mathbf{v}_c^2$ ratio could mask the effect of morphology on $K_{rot}{:}K_{trans}$. Finally, we tested for differences in the effective distance traveled to determine whether the three morphotypes differed in their tendency toward directed movement on the differing substrates. Effective distance was defined as the net distance traveled over the

20h period divided by the total distance traveled. Therefore, effective distance values close to one would indicate strong directional preference. Our models for $K_{rot}{:}K_{trans}$, $\boldsymbol{\omega}^2{:}\mathbf{v}_c^2$ and effective distance traveled (D_{eff}) as dependent variables were:

$$K_{rot}{:}K_{trans} = \beta_0 + \beta_1 x_t + \beta_2 x_s + \beta_3 x_r \ , \tag{12}$$

$$\boldsymbol{\omega}^2{:}\mathbf{v}_c^2 = \beta_0 + \beta_1 x_t + \beta_2 x_s + \beta_3 x_r \tag{13}$$

and

$$D_{eff} = \beta_0 + \beta_1 x_t + \beta_2 x_s + \beta_3 x_r \ , \tag{14}$$

where independent variables were represented by mussel morphotype (x_t), substrate type (x_s) and replicate (x_r). Maximum likelihood parameter estimates were represented by β_0, β_1, β_2 and β_3. All variables were treated as fixed effects.

We also tested whether the polar moment of inertia depended on mussel morphotype and mussel mass using an ANOVA, with Tukey's *post hoc* pairwise comparisons, in R. We tested for differences in polar moment of inertia among the morphotypes used in the locomotion analysis (from Lake Michigan) to determine whether shell morphology was correlated with locomotion. As the mussel populations used to collect morphometric data above were from Lake Ontario, this additional morphometric analysis was necessary for Lake Michigan samples. We also tested for differences in mass among morphotypes using an ANOVA, with Tukey's *post hoc* pairwise comparisons, to confirm that all mussels were of similar size.

We tested for differences in orientation of the three morphotypes during movement on hard glass and soft sedimentary substrates using logistic regression in R with Tukey's *post hoc* pairwise comparisons.
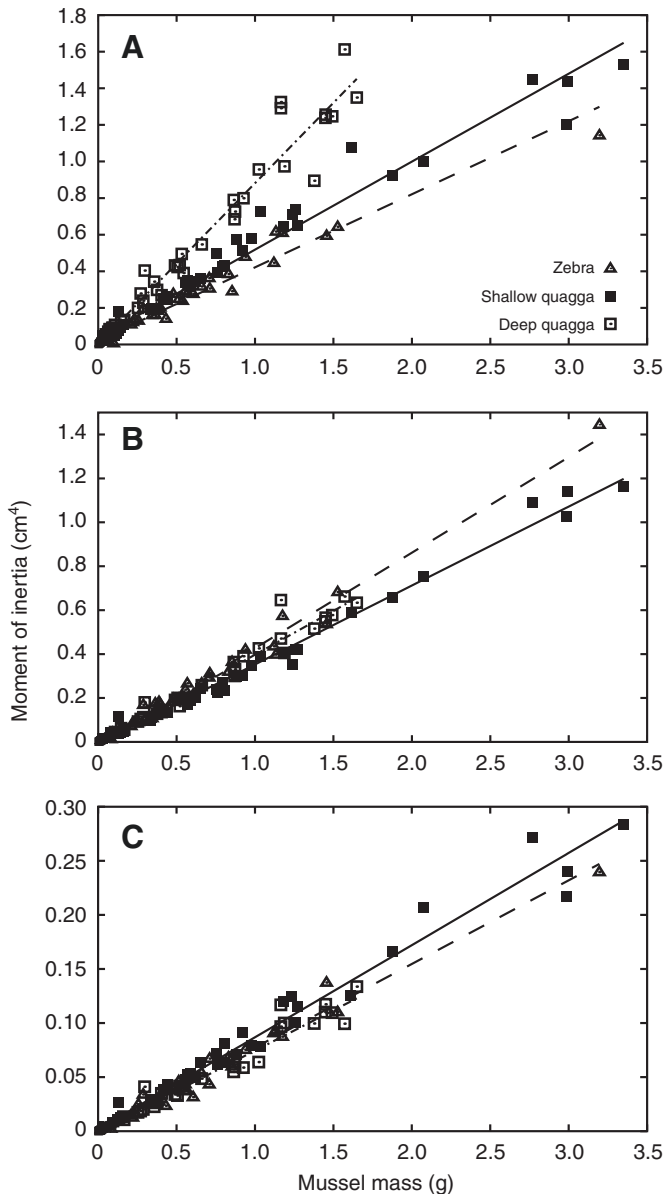
Fig. 6. Differences in polar moment of inertia among morphotypes [zebra (dashed line), shallow quagga (solid line), deep quagga mussels (dot-dashed line)] across mass, shown for the (A) lateral (J_{zz}), (B) dorsal–ventral (J_{yy}) and (C) anterior–posterior (J_{xx}) shell views (see Fig. 2). $N=60$ for each morphotype. Mussel mass was raised to the 4/3 power to non-dimensionalize its relationship with J_{zz}, J_{yy} and J_{xx}.

Fig. 7. Differences in mechanics of motion among morphotypes on different substrate types (i.e. hard glass *versus* soft sediment) (***, $P<0.001$). Mechanics of mussel motion was measured as mean ratio of rotational to translational kinetic energy ($K_{rot}:K_{trans}$). On glass substrate, $N=32$ for zebra, $N=30$ for shallow quagga and $N=26$ for deep quagga mussels. On soft sedimentary substrate, $N=24$ per morphotype. Error bars are ±s.e.m.

The model for percentage of steps of each walk, p, for which a mussel was orientated with its lateral, dorsal–ventral or anterior–posterior shell view parallel to the substrate was:

$$p = \frac{e^{\beta_0 + \beta_1 x_t + \beta_2 x_r}}{1 + e^{\beta_0 + \beta_1 x_t + \beta_2 x_r}}, \tag{15}$$

with mussel morphotype (x_t) and replicate (x_r) as independent variables. Maximum likelihood parameter estimates were represented by β_0, β_1 and β_2. Our model used a logit link function, because our data consisted of proportions, and quasibinomial errors to account for overdispersion. Our independent variables, x_t and x_r, were treated as fixed effects.
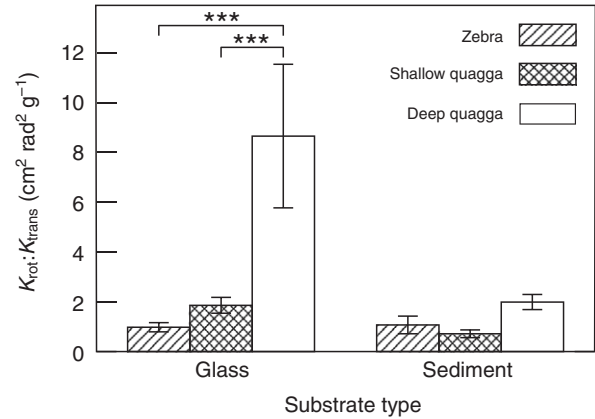
RESULTS

Moment of inertia of zebra and quagga mussel morphotypes

Shell morphology, quantified by the polar moment of inertia, differed significantly among the three morphotypes (i.e. zebra, shallow quagga and deep quagga) for all three shell views (Fig. 6, Table 1). Distribution of shell area and resistance to rotation about the z-axis (Fig. 2A, lateral shell view J_{zz}) was greatest for deep quagga mussels relative to the other morphotypes [assuming $\rho(\mathbf{r})=m/V$ in Eqn 1] for a given mass (Fig. 6A; Table 1, comparisons 1, 2; Eqn 5). Therefore, greater work was required by deep quagga mussels than by zebra or shallow quagga mussels to turn a given amount (of degrees or radians) about the z-axis for a given mass (Fig. 2A, J_{zz} only). However, distribution of shell area and presumed resistance to rotation about the y-axis (Fig. 2B, dorsal–ventral shell view J_{yy}) was greatest for zebra mussels (Fig. 6B; Table 1, comparisons 4, 5; Eqn 6), indicating greater work required by zebra mussels to turn a given amount about the y-axis (Fig. 2B, J_{yy} only). Finally, resistance to rotation about the x-axis (Fig. 2C, anterior–posterior shell view J_{xx}) was greatest for shallow quagga mussels relative to the other morphotypes (Fig. 6C; Table 1, comparisons 7, 8; Eqn 7), indicating greater work for shallow quagga mussels to turn about the x-axis (Fig. 2C, J_{xx} only).

In addition to the morphometric analysis above, using mussels collected from Lake Ontario, we performed an additional comparison of morphotypes that were independently collected (from Lake Michigan) for the locomotion analysis. This second data set of mussels possessed a narrower size range. Results from the Lake Michigan samples were concordant with those above, except that deep quagga mussels showed significantly greater J_{yy} (dorsal–ventral shell view) for a given mass than the other morphotypes (Table 2, comparisons 4, 5). The deep quagga mussels from Lake Michigan were visibly longer than those from Lake Ontario, which would account for their greater J_{yy}. The different morphotypes from Lake Michigan did not differ significantly in mass (ANOVA: $F=0.88$, d.f.=2, $P=0.42$), indicating that differences in mass were unlikely to contribute to differences in locomotion between the morphotypes.

Table 1. Pairwise comparisons of polar moment of inertia between mussel morphotypes (zebra, shallow quagga and deep quagga), for lateral, dorsal–ventral and anterior–posterior shell views (Eqns 5–7; d.f.=175)

Shell view	Comparison	Student's t	P-value	Eqn
Lateral (J_{zz})	(1) Deep quagga *versus* shallow quagga	19.5	<0.00001	5
	(2) Deep quagga *versus* zebra	20.1	<0.00001	5
	(3) Shallow quagga *versus* zebra	4.23	0.00011	5
Dorsal–ventral (J_{yy})	(4) Zebra *versus* deep quagga	3.59	0.0013	6
	(5) Zebra *versus* shallow quagga	9.15	<0.00001	6
	(6) Deep quagga *versus* shallow quagga	4.47	0.000042	6
Anterior–posterior (J_{xx})	(7) Shallow quagga *versus* zebra	3.79	0.00063	7
	(8) Shallow quagga *versus* deep quagga	4.88	<0.00001	7
	(9) Zebra *versus* deep quagga	1.06	0.87	7

Mussels were collected from Lake Ontario and used for morphometric analyses only. Morphometric data were analysed with an ANCOVA.

Table 2. Pairwise comparisons of polar moment of inertia for a given mussel mass between mussel morphotypes for lateral, dorsal–ventral and anterior–posterior shell views

Shell view	Comparison	P
Lateral (J_{zz})	(1) Deep quagga *versus* shallow quagga	<0.00001
	(2) Deep quagga *versus* zebra	<0.00001
	(3) Shallow quagga *versus* zebra	<0.00001
Dorsal–ventral (J_{yy})	(4) Deep quagga *versus* zebra	0.0021
	(5) Deep quagga *versus* shallow quagga	<0.00001
	(6) Zebra *versus* shallow quagga	<0.00001
Anterior–posterior (J_{xx})	(7) Shallow quagga *versus* zebra	0.033
	(8) Shallow quagga *versus* deep quagga	0.00093
	(9) Zebra *versus* deep quagga	0.40

Mussels were collected from Lake Michigan and used for locomotion analyses. Morphometric data were analysed with an ANOVA. P-values are from Tukey's *post hoc* tests.

Locomotion of the three morphotypes on differing substrates

The ratio of rotational to translational kinetic energy (K_{rot}:K_{trans}) depended significantly on mussel morphotype (ANOVA: F=8.57, d.f.=2, P=0.0003) and substrate type (ANOVA: F=6.29, d.f.=1, P=0.013) but not on replicate (ANOVA: F=3.34, d.f.=1, P=0.070) (Table 3, Fig. 7). On glass substrate, K_{rot}:K_{trans} was significantly greater for deep quagga than for zebra and shallow quagga mussels (Table 3A, comparisons 1, 2; Fig. 7). In addition, deep quagga mussels had significantly greater K_{rot}:K_{trans} on glass relative to soft sedimentary substrate (Table 3B, comparison 1; Fig. 7), whereas shallow quagga and zebra mussels did not differ significantly in K_{rot}:K_{trans} between the two substrates (Table 3B, comparisons 2, 3; Fig. 7). Overall, these results indicated that deep quagga mussels expended more work in rotational relative to translational movement than either zebra or shallow quagga mussels on glass but not on soft sedimentary substrate. The ω^2:$\mathbf{v}_c^2$ ratio, a component within K_{rot}:K_{trans} (Eqns 8, 9), did not differ significantly among morphotypes on each substrate (ANOVA: F=1.63, d.f.=2, P=0.20), between substrate types for each morphotype (ANOVA: F=0.43, d.f.=1, P=0.51) or among replicates (ANOVA: F=0.35, d.f.=2, P=0.56; Fig. 8). Therefore, the significant differences in K_{rot}:K_{trans} among morphotypes were caused primarily by differences in mussel shell morphology (i.e. magnitude of the polar moment of inertia) rather than by ω^2:$\mathbf{v}_c^2$, the degree of turning relative to translation of a mussel during movement.

The ratio of net to total distance traveled (i.e. effective distance) differed significantly among morphotypes (ANOVA: F=12.7, d.f.=2,

Table 3. Pairwise comparisons of rotational to translational kinetic energy (K_{rot}:K_{trans}) (A) between mussel morphotypes on hard (glass) and sedimentary substrates and (B) between substrate types for each morphotype

	Comparison	P
(A) Substrate		
Glass	(1) Deep quagga *versus* zebra	0.000055
	(2) Deep quagga *versus* shallow quagga	0.00066
	(3) Zebra *versus* shallow quagga	0.99
Sediment	(4) Zebra *versus* shallow quagga	0.99
	(5) Zebra *versus* deep quagga	0.99
	(6) Shallow quagga *versus* deep quagga	0.98
(B) Morphotype		
Deep quagga	(1) Glass *versus* sediment	0.0024
Shallow quagga	(2) Glass *versus* sediment	0.98
Zebra	(3) Glass *versus* sediment	0.99

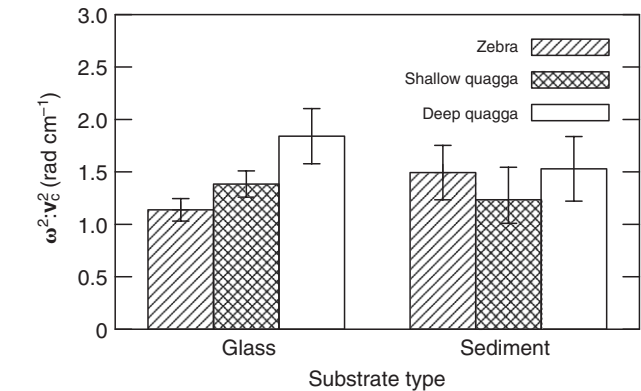P-values are from Tukey's *post hoc* tests.

Fig. 8. Differences in the amount of turning relative to translation (ω^2:$\mathbf{v}_c^2$ ratio) among morphotypes on different substrate types (glass, sediment). On glass substrate, N=32 for zebra, N=30 for shallow quagga and N=26 for deep quagga mussels. On soft sedimentary substrate, N=24 per morphotype. Error bars are ±s.e.m.
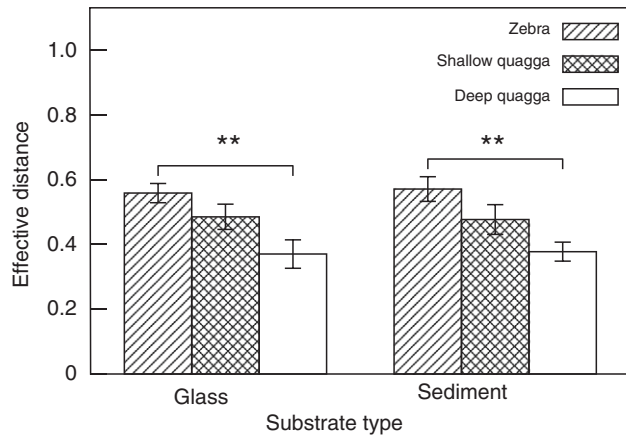
Fig. 9. Differences in effective distance traveled (i.e. ratio of net to total distance traveled) among morphotypes on different substrate types (glass, sediment) (**, $P<0.01$). On glass substrate, $N=32$ for zebra, $N=30$ for shallow quagga and $N=26$ for deep quagga mussels. On soft sedimentary substrate, $N=24$ per morphotype. Error bars are ±s.e.m.

Fig. 10. Differences in shell orientation during movement among morphotypes (***, $P<0.0001$). Graph shows percentage of steps of each 'walk' for which a mussel was positioned on its lateral, ventral and posterior (see Fig. 1) surfaces. On hard (glass) substrate, mussels were oriented in two possible positions, either on lateral (L) or ventral (D-V) surfaces. On soft sedimentary substrate, mussels were oriented in three possible positions, either on lateral, ventral or posterior (A-P) surfaces.

$P<0.00001$; Fig. 9). Zebra mussels exhibited significantly greater effective distance traveled than deep quagga mussels on glass (Tukey: $P=0.0044$) and on soft sedimentary substrates (Tukey: $P=0.0091$). Shallow quagga mussels did not differ significantly from zebra or deep quagga mussels in effective distance traveled on either substrate (Tukey: $P>0.24$). Therefore, only zebra mussels were more directed in their movement than deep quagga mussels on the two substrates. Effective distance traveled did not differ significantly for a given morphotype on the two substrates (ANOVA: $F=0.015$, d.f.=1, $P=0.90$) or among replicates (ANOVA: $F=0.93$, d.f.=1, $P=0.34$).

Mussel orientation during locomotion

During movement on glass, the morphotypes differed significantly in their orientation, with either their lateral (Fig. 2A) or ventral shell surface (Fig. 2B) towards (i.e. parallel to) the substrate. Most notably, zebra mussels were oriented with their ventral surface (from which their foot protrudes) towards the glass substrate significantly more often than deep quagga mussels (Table 4A, comparisons 1–3; Fig. 10, Fig. 11A). However, deep quagga mussels were primarily oriented with their lateral shell surface towards the glass substrate, with the foot extended out laterally, significantly more often than the other morphotypes (Fig. 10, Fig. 11A). Therefore, the polar moment of inertia of the dorsal–ventral shell view (Fig. 2B, i.e. J_{yy}) contributed primarily to $K_{rot}:K_{trans}$ of zebra mussels, whereas the polar moment of inertia of the lateral shell view (Fig. 2A, i.e. J_{zz}) mostly contributed to $K_{rot}:K_{trans}$ of deep quagga mussels.
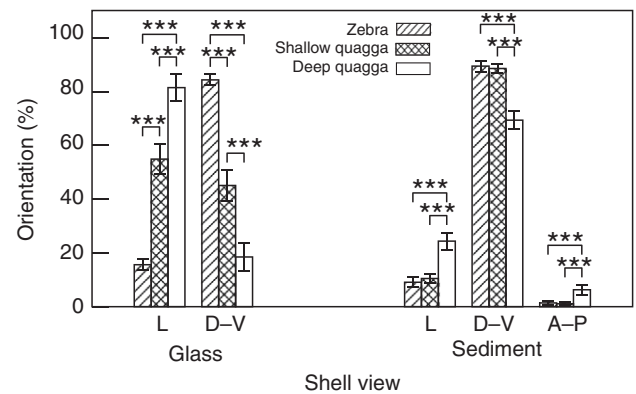
During movement on soft sediment, mussels were oriented in one of three positions, with the lateral (Fig. 2A), ventral (Fig. 2B) or posterior shell surface (i.e. hinge, Fig. 2C) towards the substrate. However, all morphotypes were oriented mostly with their ventral surface towards the substrate (Fig. 10, Fig. 11B). Zebra mussels were positioned on their ventral surface significantly more often than deep quagga mussels but did not differ significantly from shallow quagga mussels in this regard (Table 4B, comparisons 1–3; Fig. 10). Mean percentages of steps for which mussels were oriented with their ventral surface towards the substrate were greater on soft sedimentary substrate than on glass substrate for all three morphotypes (Fig. 10). Most notably, deep quagga mussels were oriented on their ventral surface for ~70% of the steps while moving on sedimentary substrate (Fig. 10) but for only ~20% of the steps while moving on glass substrate (Fig. 10). Therefore, unlike on glass substrate, on sedimentary substrate the polar moment of inertia of the dorsal–ventral shell view (i.e. J_{yy}) contributed primarily to $K_{rot}:K_{trans}$ of deep quagga mussels, similar to that of zebra and shallow quagga mussels.

DISCUSSION

Shell morphology serves as a functional trait that affects mussel locomotion on distinct substrate types. We found that shell morphology differed significantly among the three morphotypes (Figs 1, 6), and that shell morphology affected movement of the mussels differentially across hard relative to soft sedimentary substrates (Figs 7, 9). Specifically, the polar moment of inertia, our

Table 4. Pairwise comparisons of the percentage of steps of each walk where the ventral shell surface was oriented toward the substrate between mussel morphotypes (A) on glass (Eqn 15; d.f.=87) and (B) on soft sedimentary substrate (Eqn 15; d.f.=70)

Substrate	Comparison	Z	P
(A) Glass	(1) Zebra *versus* deep quagga	8.45	<0.00001
	(2) Zebra *versus* shallow quagga	5.96	<0.00001
	(3) Shallow quagga *versus* deep quagga	3.81	0.00040
(B) Sediment	(4) Zebra *versus* deep quagga	4.72	<0.00001
	(5) Zebra *versus* shallow quagga	0.16	0.98
	(6) Deep quagga *versus* shallow quagga	5.42	<0.00001

Mussel orientation did not differ significantly among replicate aquaria (glass substrate: Student's $t=-0.51$, $P=0.61$; soft sedimentary substrate: Student's $t=0.087$, $P=0.93$). P-values are from Tukey's *post hoc* tests.

descriptor of shell morphology, directly contributed to differences in work expenditure during movement on glass substrate (i.e. K_{rot}:K_{trans}) between morphotypes (i.e. deep quagga *versus* zebra and shallow quagga mussels). This effect of shell morphology on locomotion provides the first biomechanically quantifiable insights into the ability of each morphotype to interact with and colonize different substrates within the Great Lakes.

Rotational *versus* translational kinetic energy of mussels

We examined whether zebra, shallow quagga and deep quagga mussels differ in their movement (K_{rot}:K_{trans}; see Eqns 8, 9) on hard *versus* soft sedimentary substrate. High K_{rot}:K_{trans} (greater than one) indicates greater work expenditure in the form of rotation (i.e. K_{rot}; turning) relative to translation (i.e. K_{trans}; directed movement). On hard (glass) substrate, deep quagga mussels expended a significantly greater proportion of work than zebra and shallow quagga mussels in the form of rotation, with approximately fourfold greater K_{rot}:K_{trans} than zebra and shallow quagga mussels (Fig. 7). This difference in K_{rot}:K_{trans} of deep quagga relative to zebra or shallow quagga mussels was primarily attributed to the difference in the magnitude of their polar moment of inertia rather than the degree of turning relative to translating, as we found no statistically significant difference in the ω^2:v_c^2 ratio among morphotypes (Fig. 8; see Eqns 8, 9).

The extent to which the polar moment of inertia (J_{zz}, J_{yy} or J_{xx}) contributed to K_{rot}:K_{trans} (see Eqn 9) depended on shell morphology (Fig. 6) and the orientation of the mussels during movement (Figs 5, 10, 11). On glass substrate, deep quagga mussels were primarily positioned on and rotated about the axis defining their lateral shell surface (z-axis; J_{zz}) during movement (Fig. 10, Fig. 11A). Therefore, K_{rot} for deep quagga mussels was dominated by the equation:

$$K_{rot} = \frac{1}{2} m \cdot J_{zz} \cdot \omega_c^2 .$$ (16)

This lateral shell view exhibited the greatest polar moment of inertia (J_{zz}) for all morphotypes of a given mass (Fig. 6A). However, during movement on glass substrate, zebra and shallow quagga mussels were positioned on their ventral surface and rotated mostly about the axis defining their dorsal–ventral shell surface (y-axis; J_{yy}) more often than deep quagga mussels (Fig. 10, Fig. 11A). Therefore, relative to deep quagga mussels, K_{rot} for zebra and shallow quagga mussels was more dominated by the equation:

$$K_{rot} = \frac{1}{2} m \cdot J_{yy} \cdot \omega_c^2 .$$ (17)

Values of J_{yy} for the dorsal–ventral shell view for zebra and shallow quagga mussels were less than values of J_{zz} for the lateral shell view for deep quagga mussels (Fig. 6A *versus* Fig. 6B). Such greater polar moment of inertia (J_{zz}) of deep quagga mussels relative to the lesser J_{yy} of zebra and shallow quagga mussels (Eqn 16 *versus* Eqn 17) resulted in greater K_{rot}:K_{trans} for deep quagga mussels. Thus, to achieve the same amount of rotation as zebra and shallow quagga mussels on hard substrate, deep quagga mussels were required to expend a greater amount of work. In essence, the movement of deep quagga mussels was analogous to a figure skater spinning with outstretched arms, increasing the resistance to rotation, whereas the movement of zebra and shallow quagga mussels was analogous to a figure skater spinning with arms held close to the body. Even if all three morphotypes were positioned on their lateral shell surface, deep quagga mussels would still have the greatest K_{rot}:K_{trans} (assuming similar ω^2:v_c^2 among morphotypes) because they had the greatest J_{zz} (Fig. 6A). If a mussel's capacity to turn has functional and fitness consequences, deep quagga mussels might be at an
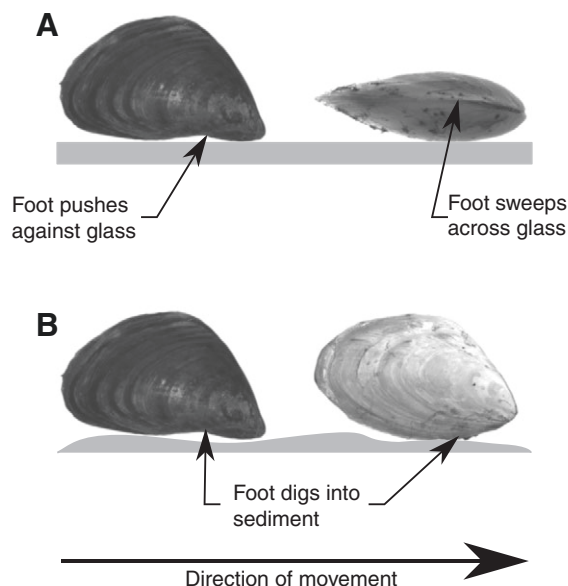
Fig. 11. Most common shell orientation and mode of locomotion of shallow (left) and deep quagga (right) mussels on (A) hard (glass) and (B) soft sedimentary substrates. Shell orientation and mode of locomotion of zebra mussels (not shown) on the two substrates were similar to that of shallow quagga mussels. All mussels were primarily positioned on their ventral shell surface on the two substrates, except for deep quagga mussels on glass substrate, which were positioned on their lateral shell surface.

energetic disadvantage, in terms of locomotion on hard substrate, as a consequence of shell morphology and mussel orientation relative to the substrate.

The similarity in energy expenditure among the three morphotypes on soft sedimentary substrate was largely due to a decrease in K_{rot}:K_{trans} of deep quagga mussels to approximately one-third of that on glass substrate (Fig. 7). Such a reduction in K_{rot}:K_{trans} of deep quagga mussels between the differing substrate types was also attributed to shell morphology and mussel orientation. Whereas on glass substrate deep quagga mussels were positioned on and rotated about their lateral shell surface (z-axis) (i.e. relatively high value for J_{zz}; Fig. 10, Fig. 11A), on soft sedimentary substrate deep quagga mussels were able to position themselves on and rotate about their ventral surface (y-axis) (i.e. relatively low value for J_{yy}; Fig. 10, Fig. 11B), similar to zebra and shallow quagga mussels. Therefore, on soft sedimentary substrate, all three morphotypes were able to minimize their polar moment of inertia with respect to the y-axis (analogous to a figure skater spinning with arms held close to the body), consequently reducing K_{rot}. In contrast to glass substrate, soft sediment appeared to provide lateral support for deep quagga mussels as they generated a path for themselves, enabling them to remain positioned on their ventral surface more often (Fig. 1C, anterior–posterior view). Consequently, deep quagga mussels were able to attain equal performance, with respect to the amount of work needed for rotation and translation, relative to zebra and shallow quagga mussels on soft sedimentary substrate.

Functional consequences of shell morphology for locomotion and other activities

We also examined whether zebra, shallow quagga and deep quagga mussels differed in their effective distance traveled on hard *versus* soft sedimentary substrate. Zebra mussels showed the greatest and

deep quagga mussels showed the lowest effective distance traveled on both hard and soft sedimentary substrates (Fig. 9). Thus, of all morphotypes, zebra mussels achieved the most directed movement in translation, although shallow quagga mussels were not significantly different from zebra mussels in terms of this aspect of locomotion.

Directed movement is likely to be a fitness-related trait that affects fitness and survival. As mentioned previously (see Introduction), zebra mussels have been found to move in response to environmental factors, including light, nitrogenous waste, oxygen and substrate type (see Burks et al., 2002; Kilgour and Mackie, 1993; Kobak, 2001; Kobak and Nowacki, 2007; Marsden and Lansky, 2000; Toomey et al., 2002). A previous study found that zebra mussels moved 22 cm within a 2 h period (Toomey et al., 2002). In our study we observed zebra, shallow quagga and deep quagga mussels moving mean distances of 20 cm (s.e.m.=0.051 cm), 29 cm (s.e.m.=0.084 cm) and 21 cm (s.e.m.=0.065 cm), respectively, within a 20 h time frame across the different substrates. Zebra mussels have also been found to seek dimmer over brighter lit habitats (Kobak, 2001; Kobak and Nowacki, 2007; Toomey et al., 2002) and show preference for specific substrate types (Kilgour and Mackie, 1993; Marsden and Lansky, 2000) and substrate color (Kobak, 2001). Other bivalves have been shown to aggregate in the presence of predators [e.g. *Mytilus edulis* (Côte and Jelnikar, 1999); see also *Tridacna squamosa* (Huang et al., 2007)]. Some (e.g. unionids) have been thought to move in response to water flow or food conditions (Schwalb and Pusch, 2007) and during spawning events (Watters et al., 2001). Thus, the ability of zebra and shallow quagga mussels to achieve greater directed movement than deep quagga mussels, in addition to the lesser energy that they expend in transit on hard substrates (i.e. lesser K_{rot}:K_{trans}), is likely to have functional benefits, possibly enabling more effective movement in response to such environmental conditions.

Achieving directed movement is likely to depend on ventral surface morphology, which is highly flattened for zebra mussels (Fig. 2A, anterior–posterior view) and appears to provide a stable platform during locomotion on flatter hard substrates. Deep quagga mussels that lack such a flattened ventral surface (Fig. 1C, anterior–posterior view) might be at a disadvantage with respect to seeking the most favorable environmental conditions in a directed manner on flat hard surfaces.

Our results suggest that shell morphology has functional consequences for mussel movement on hard *versus* soft sedimentary substrates. These consequences might contribute to differences in colonization and range expansion of zebra *versus* quagga mussels. For example, developmental plasticity has been found to contribute significantly to the divergence in shell morphology between shallow and deep quagga mussels (Peyer et al., 2010). Such a plastic response in morphology to environmental factors might allow quagga mussels greater ability than zebra mussels to utilize diverse substrates and colonize both shallow- and deep-water habitats of the Great Lakes. Although the deep quagga mussel morphotype appeared to be maladaptive with respect to movement on hard substrate (i.e. high K_{rot}:K_{trans}), the shallow quagga mussel achieved values for K_{rot}:K_{trans} that were more similar to that of the zebra mussel, resulting in similar energy expenditure between these two morphotypes (Fig. 7). In addition, values for K_{rot}:K_{trans} and effective distance traveled were not significantly different between zebra and shallow quagga mussels on both substrates (Figs 7, 9). Thus, shallow quagga mussels were similar to zebra mussels in our calculated metrics of locomotion on both hard and soft sedimentary substrates. Although deep quagga mussels had the least effective distance traveled on both substrates,

the energy that they expended in terms of K_{rot}:K_{trans} was comparable to that of zebra and shallow quagga mussels on soft sedimentary substrate. It is unclear why effective distance traveled was lowest for deep quagga mussels on soft sedimentary as well as on glass substrate. It is possible that effective distance traveled is affected by ventral surface morphology (Fig. 1, anterior–posterior view) on soft sedimentary as well as on glass substrate. Frictional forces, which our study did not take into account, might also play an important role in such movement.

Within their invaded ranges, zebra and quagga mussels come into direct contact and have direct competitive interactions in shallow-water habitats with hard substrates. Yet the colonization of deep soft sedimentary substrate by quagga mussels is also of concern, because the substrate of the Great Lakes is predominantly comprised of soft sediment [e.g. ~80% of the area in Lake Erie (Berkman et al., 1998)]. Although the deep quagga mussel morphotype appears to exact a cost to locomotion on flatter hard substrates, the shells might be adaptive for living on the soft sedimentary substrate typical of deeper waters, although studies on such effects have yet to be performed. If the deep quagga mussel shells are adaptive for living on soft sedimentary substrate, quagga mussels might have the advantage of having the ability to adopt both shallow- and deep-water morphotypes (Fig. 1B,C) [i.e. *via* developmental plasticity (Peyer et al., 2010)], providing greater versatility for utilizing both hard and soft sedimentary substrates. This versatility might confer quagga mussels with a greater ability to colonize a wider range of habitats than zebra mussels, and might lead to an overall fitness advantage in the long run.

Shell morphology might have additional functional consequences that affect the distribution of the two species. For example, the flattened ventral surface morphology of zebra mussels might aid in resisting dislodgment in flow, by enabling secure attachment with byssal threads to hard substrates in shallow-water habitats (Claxton et al., 1998; Dermott and Munawar, 1993; Mackie, 1991; Peyer et al., 2009). In addition, the high-density shells of zebra and shallow quagga mussels relative to deep quagga mussels (see Claxton et al., 1998; Roe and MacIsaac, 1997) have been considered less prone to damage in shallow-water habitats with considerable wave impact (Claxton et al., 1998). In deep-water habitats, deep quagga mussels with shells that are flattened and compressed together might be able to burrow and attach their byssal threads more deeply into the sediment, possibly anchoring themselves more securely or avoiding predation.

Numerous studies have examined various morphological features and their effects on locomotory ability of diverse animal taxa. However, a relatively small subset of these locomotion studies included an examination of different morphological attributes of shelled animals (e.g. Alexander, 1993; Amyot and Downing, 1998; Uryu et al., 1996; Waller et al., 1999). In some studies, moments of force, which depend on shell morphology, were found to affect locomotion of various gastropods (e.g. see Huryn and Denny, 1997; Okajima and Chiba, 2009). Moments of inertia have also been proposed to play an important role in locomotion of the painted turtle, *Chrysemys picta*, although these values were not specifically calculated (Rivera et al., 2006).

Most notably, we are aware of no study that has directly quantified whole-shell morphology using a geometric measure (e.g. moment of inertia) that has direct input into physical models of motion (e.g. K_{rot}:K_{trans}). In this study, we applied a unique approach by directly linking moments of inertia to the energetics of locomotion of different mussel morphotypes. Our approach indicated novel constraints of shell morphology on locomotory ability. In particular,

such constraints were revealed by the greater work expenditure on hard substrate of deep quagga mussels relative to shallow quagga and zebra mussels. These constraints might have crucially important implications for range expansions of zebra and quagga mussels onto diverse substrate types in novel environments.

LIST OF ABBREVIATIONS

A	mussel shell area
C	shell centroid
dA	differential element of shell area
D_{eff}	effective distance traveled
dV	differential element of shell volume
I_{aa}	mass moment of inertia about the a-axis
I_{xx}	moment of inertia about the principal x-axis
I_{yy}	moment of inertia about the principal y-axis
I_{zz}	moment of inertia about the principal z-axis
$\mathbf{J}$	polar moment of inertia tensor for K_{rot} (i.e. Trace[J]=\{J_{xx}, J_{yy}, J_{zz}\})
J_{xx}	polar moment of inertia about the principal x-axis
J_{yy}	polar moment of inertia about the principal y-axis
J_{zz}	polar moment of inertia about the principal z-axis
K_{rot}	rotational kinetic energy
K_{trans}	translational kinetic energy
m	mussel mass
$\mathbf{r}$	position vector from a point on a particular axis to dA or dV
V	shell volume
$\mathbf{v}_c$	velocity of shell centroid
x	distance from y-axis to dA
x_m	mussel mass (statistical notation)
x_r	experimental replicate (statistical notation)
x_s	substrate type (statistical notation)
x_t	mussel type (statistical notation)
y	distance from x-axis to dA
β	maximum likelihood parameter estimate
$\Delta\mathbf{x}$	displacement vector of shell centroid
$\Delta\theta$	angle through which a mussel rotates
$\rho(\mathbf{r})$	density of an object at position $\mathbf{r}$ relative to a-axis
$\boldsymbol{\omega}_c$	angular velocity about instantaneous center of rotation

ACKNOWLEDGEMENTS

REFERENCES

Alexander, R. R. (1993). Correlation of shape and habit with sediment grain-size for selected species of the bivalve *Anadara*. *Lethaia* **26**, 153-162.

Amyot, J.-P. and Downing, J. A. (1998). Locomotion in *Elliptio complanata* (Mollusca: Unionidae): a reproductive function? *Freshw. Biol.* **39**, 351-358.

Beer, F. P. and Johnston, E. R., Jr (1981). *Mechanics of Materials*, 616 pp. New York: McGraw-Hill, Inc.

Berkman, P. A., Haltuch, M. A., Tichich, E., Garton, D. W., Kennedy, G. W., Gannon, J. E., Mackey, S. D., Fuller, J. A. and Liebenthal, D. L. (1998). Zebra mussels invade Lake Erie muds. *Nature* **393**, 27-28.

Burks, R. L., Tuchman, N. C., Call, C. A. and Marsden, J. E. (2002). Colonial aggregates: effects of spatial position on zebra mussel responses to vertical gradients in interstitial water quality. *J. N. Am. Benthol. Soc.* **21**, 64-75.

Carrier, D. R., Walter, R. M. and Lee, D. V. (2001). Influence of rotational inertia on turning performance of theropod dinosaurs: clues from humans with increased rotational inertia. *J. Exp. Biol.* **204**, 3917-3926.

Claxton, W. T., Wilson, A. B., Mackie, G. L. and Boulding, E. G. (1998). A genetic and morphological comparison of shallow- and deep-water populations of the introduced dreissenid bivalve *Dreissena bugensis*. *Can. J. Zool.* **76**, 1269-1276.

Côté, I. M. and Jelnikar, E. (1999). Predator-induced clumping behaviour in mussels (*Mytilus edulis* Linnaeus). *J. Exp. Mar. Biol. Ecol.* **235**, 201-211.

Dermott, R. and Munawar, M. (1993). Invasion of Lake Erie offshore sediments by *Dreissena*, and its ecological implications. *Can. J. Fish. Aquat. Sci.* **50**, 2298-2304.

Gelembiuk, G. W., May, G. E. and Lee, C. E. (2006). Phylogeography and systematics of zebra mussels and related species. *Mol. Ecol.* **15**, 1033-1050.

Hibbeler, R. C. (1989). *Engineering Mechanics: Dynamics*, 552 pp. New York: Macmillan Publishing Company.

Huang, D., Todd, P. A. and Guest, J. R. (2007). Movement and aggregation in the fluted giant clam (*Tridacna squamosa* L.). *J. Exp. Mar. Biol. Ecol.* **342**, 269-281.

Huryn, A. D. and Denny, M. W. (1997). A biomechanical process explaining upstream movements by the freshwater snail *Elimia*. *Funct. Ecol.* **11**, 472-483.

Jarvis, P., Dow, J., Dermott, R. and Bonnell, R. (2000). Zebra (*Dreissena polymorpha*) and quagga mussel (*Dreissena bugensis*) distribution and density in Lake Erie, 1992-1998. *Can. Tech. Rep. Fish. Aquat. Sci.* **2304**, 1-46.

Karatayev, A. Y., Burlakova, L. E. and Padilla, D. K. (1998). Physical factors that limit the.distribution and abundance of *Dreissena polymorpha* (Pall.). *J. Shellfish Res.* **17**, 1219-1235.

Kilgour, B. W. and Mackie, G. L. (1993). Colonization of different construction materials by the zebra mussel (*Dreissena polymorpha*). In *Zebra Mussels: Biology, Impacts, and Control* (ed. T. F. Nalepa and D. W. Schloesser), pp. 167-173. Boca Raton: CRC Press, Inc.

Kobak, J. (2001). Light, gravity and conspecifics as cues to site selection and attachment behaviour of juvenile and adult *Dreissena polymorpha* Pallas, 1771. *J. Molluscan Stud.* **67**, 183-189.

Kobak, J. and Nowacki, P. (2007). Light-related behavior of the zebra mussel (*Dreissena polymorpha*, Bivalvia). *Fund. Appl. Limnol.* **169**, 341-352.

Mackie, G. L. (1991). Biology of the exotic zebra mussel, *Dreissena polymorpha*, in relation to native bivalves and its potential impact in Lake St. Clair. *Hydrobiologia* **219**, 251-268.

Marsden, J. E. and Lansky, D. M. (2000). Substrate selection by settling zebra mussels, *Dreissena polymorpha*, relative to material, texture, orientation, and sunlight. *Can. J. Zool.* **78**, 787-793.

May, G. E., Gelembiuk, G. W., Panov, V. E., Orlova, M. I. and Lee, C. E. (2006). Molecular ecology of zebra mussel invasions. *Mol. Ecol.* **15**, 1021-1031.

Mills, E. L., Dermott, R. M., Roseman, E. F., Dustin, D., Mellina, E., Conn, D. B. and Spidle, A. P. (1993). Colonization, ecology, and population structure of the "quagga" mussel, (Bivalvia:Dreissenidae) in the lower Great Lakes. *Can. J. Fish. Aquat. Sci.* **50**, 2305-2314.

Mills, E. L., Rosenberg, G., Spidle, A. P., Ludyanskiy, M., Pligin, Y. and May, B. (1996). A review of the biology and ecology of the quagga mussel (*Dreissena bugensis*), a second species of freshwater dreissenid introduced to North America. *Am. Zool.* **36**, 271-286.

Mills, E. L., Chrisman, J. R., Baldwin, B., Owens, R. W., O'Gorman, R., Howell, T., Roseman, E. F. and Raths, M. K. (1999). Changes in the dreissenid community in the lower Great Lakes with emphasis on southern Lake Ontario. *J. Great Lakes Res.* **25**, 187-197.

Okajima, R. and Chiba, S. (2009). Cause of bimodal distribution in the shape of a terrestrial gastropod. *Evolution* **63**, 2877-2887.

Peyer, S. M., McCarthy, A. J. and Lee, C. E. (2009). Zebra mussels anchor byssal threads faster and tighter than quagga mussels in flow. *J. Exp. Biol.* **212**, 2027-2036.

Peyer, S. M., Hermanson, J. C. and Lee, C. E. (2010). Developmental plasticity of shell morphology in quagga mussels from shallow and deep-water habitats in the Great Lakes. *J. Exp. Biol.* **213**, 2602-2609.

Pimentel, D., Zuniga, R. and Morrison, D. (2005). Update on the environmental and economic costs associated with alien-invasive species in the United States. *Ecol. Econ.* **52**, 273-288.

R Development Core Team. (2008). *R: A Language and Environment for Statistical Computing.* Vienna: R Foundation for Statistical Computing.

Rivera, G., Rivera, A. R. V., Dougherty, E. E. and Blob, R. W. (2006). Aquatic turning performance of painted turtles (*Chrysemys picta*) and functional consequences of a rigid body design. *J. Exp. Biol.* **209**, 4203-4213.

Roe, S. L. and MacIsaac, H. J. (1997). Deepwater population structure and reproductive state of quagga mussels (*Dreissena bugensis*) in Lake Erie. *Can. J. Fish. Aquat. Sci.* **54**, 2428-2433.

Schwalb, A. N. and Pusch, M. T. (2007). Horizontal and vertical movements of unionid mussels in a lowland river. *J. N. Am. Benthol. Soc.* **26**, 261-272.

Stoeckmann, A. (2003). Physiological energetics of Lake Erie dreissenid mussels: a basis for the displacement of *Dreissena polymorpha* by *Dreissena bugensis*. *Can. J. Fish. Aquat. Sci.* **60**, 126-134.

Toomey, M. B., McCabe, D. and Marsden, J. E. (2002). Factors affecting the movement of adult zebra mussels (*Dreissena polymorpha*). *J. N. Am. Benthol. Soc.* **21**, 468-475.

Uryu, Y., Iwasaki, K. and Hinoue, M. (1996). Laboratory experiments on behaviour and movement of a freshwater mussel, *Limnoperna fortunei* (Dunker). *J. Molluscan Stud.* **62**, 327-341.

Vanderploeg, H. A., Liebig, J. R. and Gluck, A. A. (1996). Evaluation of different phytoplankton for supporting development of zebra mussel larvae (*Dreissena polymorpha*): the importance of size and polyunsaturated fatty acid content. *J. Great Lakes Res.* **22**, 36-45.

Waller, D. L., Gutreuter, S. and Rach, J. J. (1999). Behavioral responses to disturbance in freshwater mussels with implications for conservation and management. *J. N. Am. Benthol. Soc.* **18**, 381-390.

Walter, R. M. and Carrier, D. R. (2002). Scaling of rotational inertia in marine rodents and two species of lizard. *J. Exp. Biol.* **205**, 2135-2141.

Watters, G. T., O'Dee, S. H. and Chordas, S. (2001). Patterns of vertical migration in freshwater mussels (Bivalvia: Unionoida). *J. Freshw. Ecol.* **16**, 541-549.